

Molecular Switch Based on a Biologically Important Redox Reaction

Ping Yan, Michael W. Holman, Paul Robustelli, Arindam Chowdhury, Fady I. Ishak, and David M. Adams*

Department of Chemistry, Columbia University, 3000 Broadway, New York, New York 10027

Received: September 16, 2004; In Final Form: October 11, 2004

Building on our earlier report of a single-molecule probe,¹ we show how biologically important redox centers, nicotinamide and quinone, incorporated into a fluorophore–spacer–receptor molecular structure, form redox active molecular switches, with the photoinduced electron-transfer behavior of each depending on the oxidation state of the receptor subunit. The switch based on nicotinamide (**3/6**) is strongly fluorescent in its oxidized state ($\Phi_F \approx 1.0$) but nonfluorescent in the reduced state ($\Phi_F < 0.001$) due to electron transfer from the reduced nicotinamide to the photoexcited fluorophore. The fluorescence can be reversibly switched off and on chemically by successive reduction with NaBH_3CN and oxidation with tetrachlorobenzoquinone and switched electrochemically over 10 cycles without significant degradation. A similar switch based on quinonimine turned out to be nonfluorescent in both reduced and oxidized states: in addition to a similar quenching mechanism in the reduced state, quenching also occurs in the oxidized state, due to electron transfer from the fluorophore to the receptor. Ab initio quantum chemical calculations of orbital energy levels were used to corroborate these quenching mechanisms. Calculations predicted photoinduced electron transfer to be energetically favorable in all cases where quenching was observed and unfavorable in all cases where it was not. Application of the perylene analogue as a biosensor has also been demonstrated by coupling the switch to the catalytic pathway of yeast alcohol dehydrogenase, a common NADH/NAD^+ -utilizing enzyme.

Introduction

Molecular switches²—molecules whose optical or electronic properties change dramatically in response to an environmental perturbation—have been extensively studied and developed due to interest in their potential applications as molecular memories,^{3,4} molecular valves,⁵ and biological or chemical sensors.^{1,6} Fluorescent switches are of special interest since they allow for sensitive detection and monitoring, even down to the level of single molecules in solution and on surfaces under ambient conditions.^{1,7–9} A common motif in fluorescent switches is photoinduced electron transfer (PET)¹⁰—in the off state of the switch, PET either to or from the fluorophore quenches the fluorescence. Since these switches are based on the modulation of electron transfer, they are also of interest in the realm of molecular electronics.^{11–13} Sensors based on PET^{6,14–20} have been successfully designed for a wide variety of chemical species, including cations such as Ca^{2+} ,²¹ Zn^{2+} ,^{22,23} and Hg^{2+} ,^{24,25} anions such as pyrophosphate²⁶ and azide ion,²⁷ and neutral molecules such as amino acids²⁸ and saccharides.²⁹ While many fluorescent sensors for cations are now commercially available,³⁰ switches based on reversible redox reactions are fewer and less well-studied.^{17,31–35}

We have previously reported a molecule ($\Phi_F < 0.01$), *N*-(1-nonyldecyl)-*N'*-(*p*-aminophenyl)-perylene-3,4,9,10-tetracarboxylbisimide (NDAPP, Figure 1a) suitable for single molecule level sensing and imaging that becomes strongly fluorescent ($\Phi_F \approx 1.0$) upon protonation or coordination to a metal ion or surface.¹ The general mechanism in Figure 1d is typical for a PET-based fluorescence switch: the highest-occupied molecular orbital (HOMO) of the receptor subunit (here the free amine) is higher in energy than the HOMO of the fluorophore subunit,

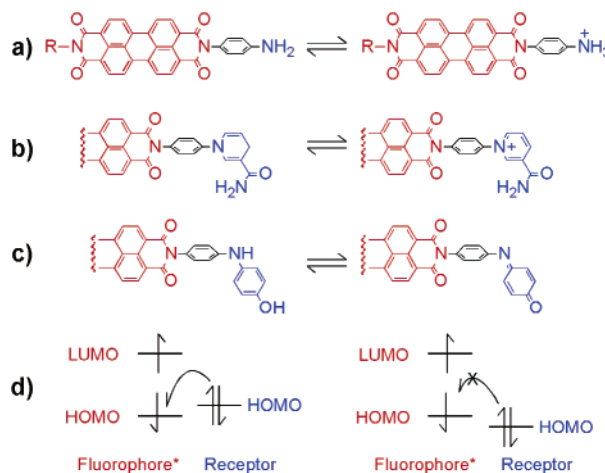
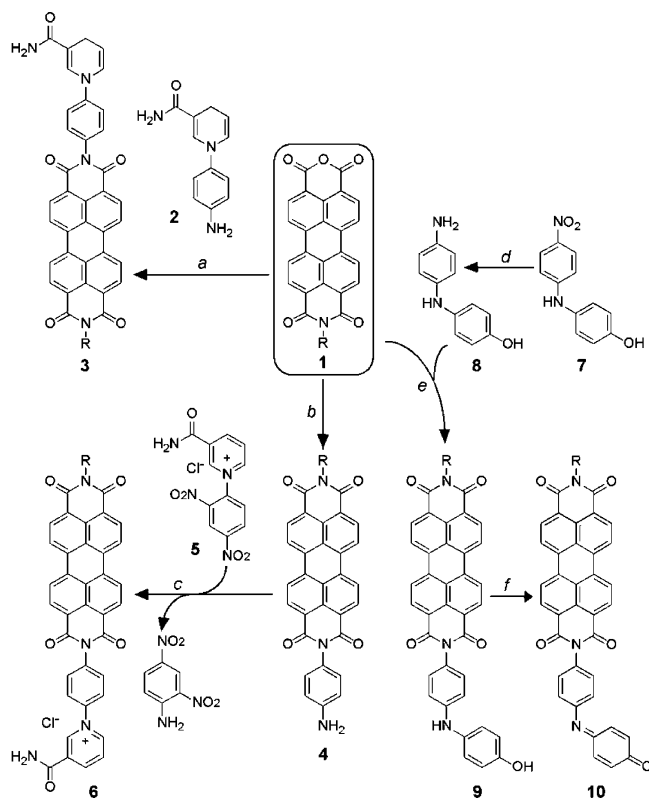


Figure 1. Fluorescence switch design based on photoinduced electron transfer: (a) aromatic amine as proton receptor, $\text{R} = -\text{CH}(n-\text{C}_9\text{H}_{19})_2$; (b) nicotinamide as redox receptor; (c) quinonimine as redox receptor; and (d) general molecular orbital diagram—the position of the receptor HOMO relative to the HOMO of the photoexcited fluorophore determines whether PET is thermodynamically favorable.

so photoexcitation of the fluorophore leads to rapid PET from the amine to the fluorophore, quenching the fluorescence. After protonation, on the other hand, the HOMO of the amine is lower than the HOMO of the fluorophore, so PET quenching is thermodynamically unfavorable, and the excited fluorophore can relax radiatively.

Here, we report a rational design of a redox switch analogous to the NDAPP proton sensor. Since part of the motivation for redox switches of fluorescence is for real-time visualization of cellular events,³⁶ two biologically important redox centers were chosen here as the redox receptors: nicotinamide, the redox

* Corresponding author. E-mail: dadams@chem.columbia.edu.

SCHEME 1^a

^a R = $-\text{CH}(n\text{-C}_6\text{H}_{13})_2$, conditions: (a) imidazole, 100 °C, 78%; (b) imidazole, 130 °C, 90%; (c) MeOH, 65 °C, 41%; (d) Pd/C, H₂, RT, 76%; (e) imidazole, 130 °C, 37%; and (f) CHCl₃, NaClO, RT, 38%. center in the ubiquitous nicotinamide adenine dinucleotide (NADH/NAD⁺), and nicotinamide adenine dinucleotide phosphate (NADPH/NADP⁺) redox couples; and quinone, which also plays an important role in cellular electron-transfer reactions.³⁷ Redox switches incorporating nicotinamide and quinonimine redox receptors are shown in Figure 1b and 1c, respectively. As in the case of NDAPP, the HOMO of an aromatic amine is higher than the HOMO of the fluorophore, and the reduced forms are nonfluorescent due to PET quenching (Figure 1d); after oxidation, the HOMO of the receptor subunit is lower than HOMO of the fluorophore, and this PET quenching no longer occurs. This paper represents a general strategy of converting amine-based cation sensors to redox active switches and sensors that can be easily coupled to enzymatic reactions.

Results and Discussion

Synthesis. Shown in Scheme 1 are the synthetic pathways for both reduced and oxidized forms of the redox switches: NADH analogue **3** and NAD⁺ analogue **6** and hydroquinonimine **9** and quinonimine **10**. Nonsymmetric perylene bisimide dyes are generally synthesized by condensation of a perylene-3,4,9,10-tetracarboxyl-3,4-anhydride-9,10-imide **1** with appropriate amines.³⁸ The long-chain secondary alkyl group in **1** improves the solubility of the products in organic solvents; other side chains could be chosen to make the products water soluble. The amines for the reduced forms, **2** and **8**, are very reactive and can condense with **1** straightforwardly. The oxidized forms were synthesized indirectly: quinonimine **10** was prepared by oxidizing the reduced form **9** with NaClO; NAD⁺ analogue **3** was synthesized by a pyridinium exchange reaction between 3-(carbamoyl)-1-(2,4-dinitrophenyl)-pyridinium chloride (**5**) and *N*-(4-aminophenyl)-*N'*-(1-hexylheptyl)-peryene-3,4,9,10-tetra-

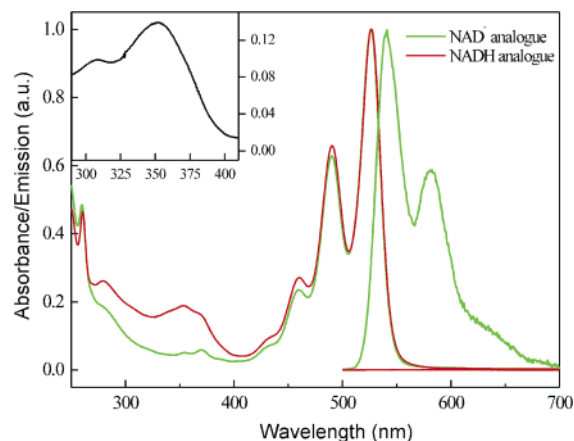


Figure 2. Comparison of normalized absorption and emission spectra of the NAD⁺ analogue and NADH analogue in 2:1 MeOH/CH₂Cl₂. The inset shows the difference in absorption between NAD⁺ and NADH analogues.

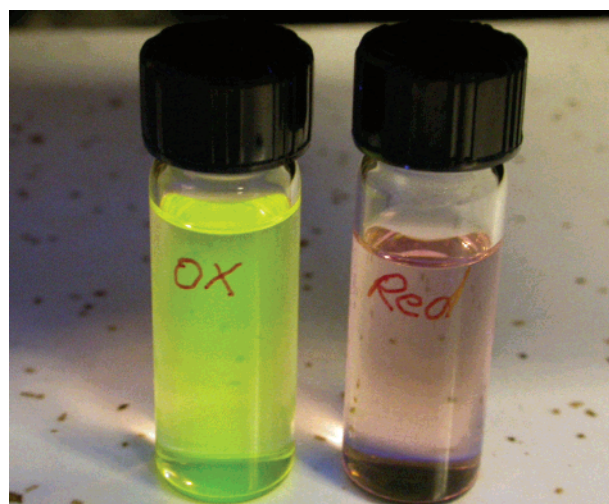


Figure 3. Photograph showing different fluorescence properties for 5 μM oxidized form (**6**), left, and reduced form (**3**), right, in 2:1 MeOH/CHCl₃.

carboxylbisimide (**4**), which in turn was synthesized by condensation of phenylenediamine with **1**.¹

Optical Properties. The absorption and fluorescence spectra of NAD⁺ analogue **6** and NADH analogue **3** are shown in Figure 2. The absorption bands above ~450 nm are identical and characteristic of perylene bisimide absorption; the absorption difference spectrum between 300 and 400 nm (Figure 2, inset) shows a strong peak at 350 nm, which is characteristic of 1,4-dihydronicotinamide and has been widely used in assays for NAD(P)H-utilizing enzymes.³⁹ Despite the similarity in absorption spectra, the fluorescence properties are very different: NAD⁺ analogue is strongly fluorescent ($\Phi \approx 1$) while the NADH analogue has almost no fluorescence ($\Phi < 0.001$). Figure 3 illustrates this difference, showing the reduced and oxidized forms in solution under UV excitation.

The other redox pair **9/10**, also has similar absorption spectra, but while the reduced form (**9**) is nonfluorescent as expected from the model in Figure 1, here the oxidized form (**10**) was also found to be nonfluorescent. We believe this is also due to PET, but now from the photoexcited fluorophore to the quinonimine, as described in detail later.

Chemical Redox Switching of Fluorescence. Reversible chemical switching requires a careful selection of reductant and oxidant: (a) the redox reaction should be selective so that the

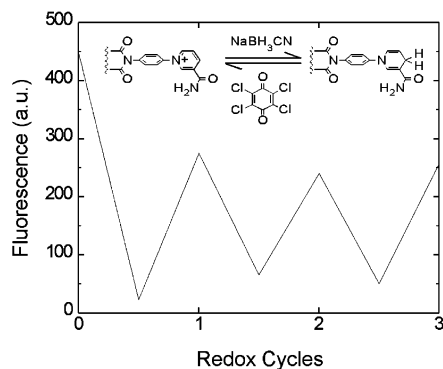


Figure 4. Variation in the fluorescence intensity for **3/6** upon repeated reduction with NaBH₃CN and oxidation with TCBQ, over three cycles.

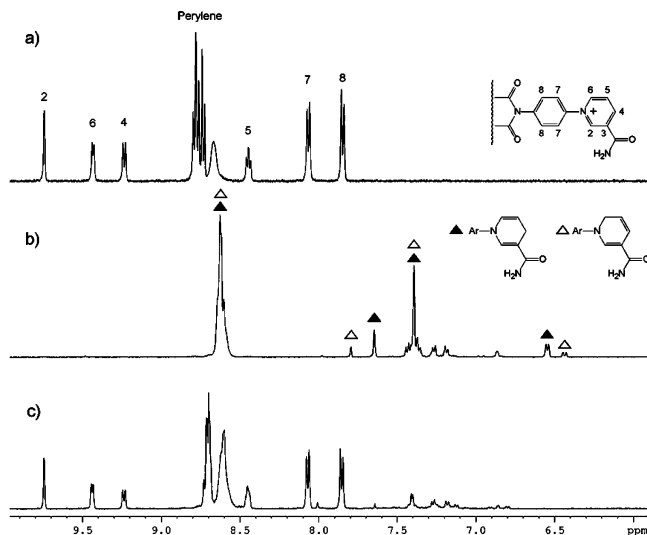


Figure 5. ¹H NMR of **6** in 1:1 CD₂Cl₂/CD₃OD: (a) before reduction; (b) after reduction with NaBH₃CN (▲, 1,4-dihydro isomer; △, 1,6-dihydro isomer); and (c) after reoxidation with TCBQ.

fluorophore is not destroyed, (b) the reaction should be clean and the byproduct should not affect further switching or quench the fluorescence, and (c) the oxidation and reduction should be carried out under similar conditions (solvent, pH, temperature). As a result, reversible chemical switching is rare in the literature, and investigators typically resort to photochemical and electrochemical methods for reversible switching. The redox interconversion between NAD⁺ analogue and NADH analogue involves two electrons and one proton, which is equivalent to a hydride (H⁻) transfer, so a hydride donor NaBH₃CN and hydride acceptor, tetrachlorobenzoquinone (TCBQ), were selected for reversible reduction and oxidation, respectively. NaBH₃CN is also known to be a selective reducing reagent for pyridinium salt in the presence of carbonyl groups.⁴⁰ TCBQ has been used successfully for the oxidation of dihydronicotinamides at room temperature, and it has been shown that this oxidation can be further accelerated by UV irradiation since the photoexcited TCBQ is a more powerful oxidant.⁴¹ The changes in fluorescence intensity for **3/6** upon repeated reduction with NaBH₃CN and oxidation with TCBQ over three cycles are shown in Figure 4.

NMR experiments confirm that the switching is between the expected products **3** and **6** (Figure 5). After reduction of the NAD⁺ analogue **6** (Figure 5a) with NaBH₃CN, the major product is clearly the NADH analogue **3** (Figure 5b), from comparison of this spectrum to the spectrum of independently prepared **3**, and the minor product is a 1,6-dihydro isomer. Both products are apparently nonfluorescent, and reoxidation gives

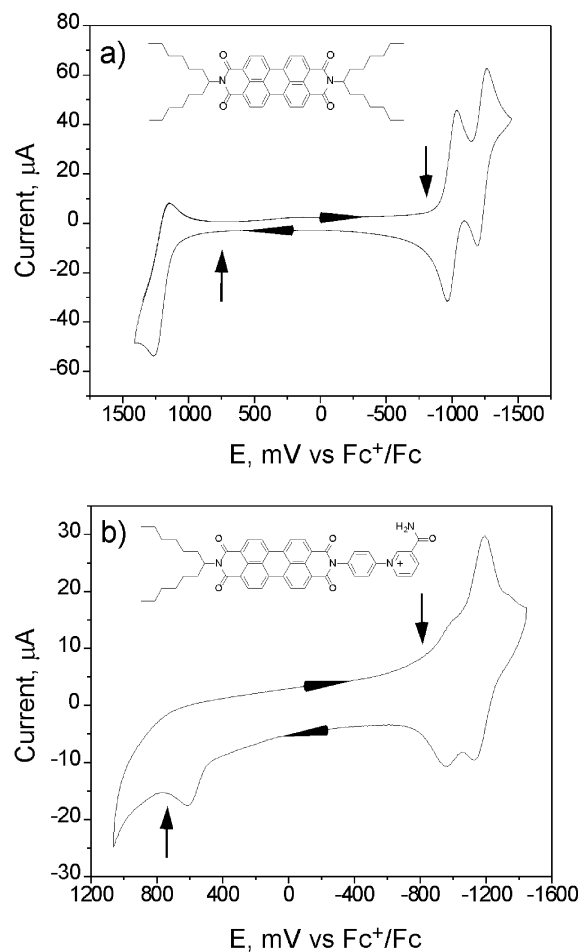


Figure 6. Cyclic voltammograms at a scan rate of 100 mV/s: (a) 0.3 mM *N,N'*-bis(1-hexylheptyl)perylene-3,4:9,10-tetracarboxylbisimide and (b) 0.1 mM **6**. Reduction/oxidation potentials used in the spectroelectrochemistry are indicated by the vertical arrows.

conversion back to the original NAD⁺ analogue **6** (Figure 5c) in ~80% yield.

Electrochemical Redox Switching of Fluorescence. To increase the understanding of biological electron-transfer reactions, intensive research efforts have been made on the electrochemistry of NAD⁺/NADH and their analogues.⁴² NAD⁺/NADH and their analogues are infamous for their electrochemical irreversibility: the two forms can be interconverted but only with large over-potentials,^{43–45} which reflects the bistability of the reduced and oxidized forms, a necessary property of a molecular switch.³ It has also often been found that NAD⁺ (or its analogues) forms dimeric products—in which a C–C bond between two nicotinamide units is formed in lieu of the new C–H bond—when reduced on a naked electrode (rather than a mediator or enzyme-modified electrode) but that the dimer can be still reoxidized back to NAD⁺ (or its analogues) at an anode wave with high over-potential.^{43–45} Figure 6 shows the cyclic voltammograms (CV) both of *N,N'*-bis(1-hexylheptyl)perylene-3,4:9,10-tetracarboxylbisimide (Figure 6a)—the fluorophore alone—and of NAD⁺ analogue **6** (Figure 6b)—both fluorophore and receptor. The CV of the ordinary perylene bisimide (Figure 6a) shows clearly one reversible oxidation and two reversible reduction peaks, in agreement with previous reports.⁴⁶ For the NAD⁺ analogue (Figure 6b), the peak for the irreversible reduction of the nicotinamide is close to the reduction peaks for the fluorophore and is not fully resolved, but the irreversible oxidation (back to the NAD⁺ analogue) is clearly distinguished at +0.6 V versus Fc⁺/Fc. The reduction product may be a dimer

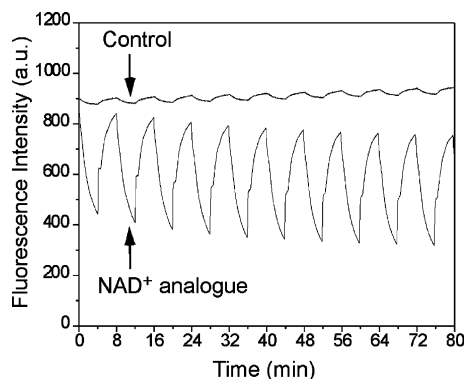


Figure 7. Reversible switching of fluorescence upon repeated electrochemical reduction/oxidation of **6** in acetonitrile. The control is *N,N'*-bis(1-hexylheptyl)perylene-3,4:9,10-tetracarboxylbisimide. The reduction and oxidation were carried out at -0.81 and $+0.76$ V vs Fc^+/Fc , respectively, for 4 min each.

or mixture of dimers rather than the NADH analogue **3**, but it is in any case nonfluorescent and is reoxidized back to the NAD^+ analogue **6**.

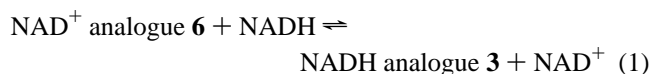
Spectroelectrochemistry was used to follow the fluorescence changes as a function of applied voltage. At a carefully selected voltage, -0.81 V versus Fc^+/Fc , the nicotinamide receptor can be reduced selectively without appreciable reduction of the fluorophore, and at $+0.76$ V versus Fc^+/Fc , the reduction product can be reoxidized cleanly. Figure 7 shows the reversible switching of fluorescence upon repeated electrochemical reduction/oxidation on the NAD^+ analogue in acetonitrile. There is about 13% degradation of the system after 10 redox cycles. *N,N'*-Bis(1-hexylheptyl)perylene-3,4:9,10-tetracarboxylbisimide, as the control, only shows small variations in fluorescence under the same conditions, probably due to a small amount of reduction of the fluorophore.

Molecular Orbital Calculations. Molecular orbital calculations have been found useful in rational design of PET probes based on benzofurazan⁴⁷ and fluorescein.^{48,49} Here, we used ab initio quantum chemical calculations to determine the relative energies of the molecular orbitals, to corroborate the quenching mechanism shown in Figure 1. We found that calculations using DFT at the B3LYP level, with a dielectric continuum solvent model (vide infra), accurately explained the observed electron-transfer behavior of the molecules studied here. Figure 8 shows the frontier molecular orbitals for the NADH and NAD^+ analogues **3** and **6**. Note that the fluorophore and the redox receptor are sufficiently decoupled that molecular orbitals are localized on either one or the other, due to the large (ca. 70°) interplanar angle between the bisimide and the phenylene moieties and to the node in the HOMO and LUMO of the perylene bisimide on the linking nitrogen atom.⁵⁰ The molecular orbitals in general are localized on either the fluorophore or the receptor and have similar contours to those calculated for an isolated perylene bisimide or isolated phenylnicotinamide. These molecular orbital calculations support the proposed quenching mechanism: in the NADH analogue (Figure 8a), the HOMO of the receptor is higher in energy than the HOMO of the fluorophore and can donate an electron to the excited state of the fluorophore to quench its fluorescence; while in the NAD^+ analogue (Figure 8b), the HOMO of the receptor is lower than the HOMO of the fluorophore and quenching via electron transfer is not energetically favorable.

Similar calculations on the quinonimine-based molecules **9** and **10** produced similar results: the molecular orbitals were found to be localized on either fluorophore or receptor and to

resemble the orbitals of the isolated species. Here also, in the reduced species the HOMO of the hydroquinonimine was found to be higher in energy than the HOMO of the fluorophore, predicting quenching by electron transfer, while the HOMO of the oxidized quinonimine was lower in energy than the HOMO of the fluorophore, predicting no quenching, as in the NADH/ NAD^+ analogues. Recall, however, that while the hydroquinonimine **9** was nonfluorescent as expected, the oxidized form **10** was also found to be nonfluorescent. The frontier molecular orbital energies plotted in Figure 9 illustrate why: in the oxidized species (Figure 9b), the LUMO of the receptor is now lower in energy than the LUMO of the perylene, so the fluorescence can now be quenched by electron transfer from the fluorophore to the receptor. Instead of switching electron transfer on and off, as with the NADH/ NAD^+ analogues, here the redox reaction changes the direction of electron transfer. While potentially also of interest, this process is not so amenable to study via fluorescence spectroscopy. Note (Figure 8b) that the calculations correctly predict that this reversed electron-transfer quenching cannot occur for the NAD^+ analogue because there the LUMO of the receptor is still higher in energy than the LUMO of the fluorophore.

Coupling the Redox Switch to an Enzymatic Pathway. As a first step toward combinatorial screening and cellular imaging, we coupled the redox switch to a catalytic enzymatic reaction utilizing NADH/ NAD^+ cofactors, as shown in Figure 10a. The redox potential of **3/6**, which is difficult to ascertain precisely from the electrochemical measurements, is only slightly perturbed from that of natural NADH/ NAD^+ . We studied the equilibrium reaction (eq 1) of **3/6** with NADH/ NAD^+ in two different limiting environments: organic solution involving acetonitrile/ H_2O (97:3) and aqueous solution involving micelles



Addition of 6 equiv of NADH to **6** in acetonitrile ($1.6 \mu\text{M}$) resulted in an 85% decrease in fluorescence. Similarly, in an aqueous environment, where **6** was solubilized by *n*-dodecyl- β -D-maltoside (DDM) and the reaction was facilitated by a phase transfer catalyst, cetyltrimethylammonium bromide (CTAB), **6** could be easily reduced by NADH. The reverse reaction, involving addition of NAD^+ to **3**, gave an insignificant increase in fluorescence, suggesting that the oxidation of **3** with NAD^+ is not energetically favorable and that the equilibrium in eq 1 lies to the right.

While **3/6** is too sterically hindered to be bound by the enzyme directly, this NADH cross-reaction allows us to couple any enzymatic reaction that produces NADH to our fluorescent switch. Figure 10a shows this process for a typical NADH/ NAD^+ -utilizing enzyme, yeast alcohol dehydrogenase (ADH). ADH catalyzes the oxidation of ethanol to acetaldehyde as NAD^+ is reduced to NADH. Coupling the reaction in eq 1 into this biochemical pathway allows for detection of the enzymatic turnover. Figure 10b shows the change in fluorescence versus time for a micellar aqueous solution of probe (**6**), enzyme (ADH), substrate (ethanol), and cofactor (NAD^+). Fluorescence intensity (■) decreases as the probe monitors the production of NADH due to the enzymatic reaction. In control experiments, where the enzymatic cycle is halted by leaving out either NAD^+ (●), ADH (▲), or ethanol (★), little fluorescence change is observed.

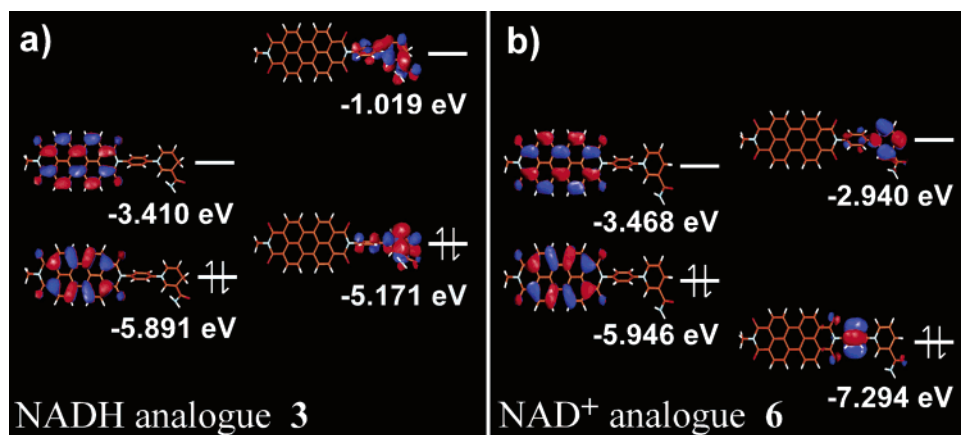


Figure 8. Frontier molecular orbitals for (a) NADH analogue 3 and (b) NAD⁺ analogue 6.

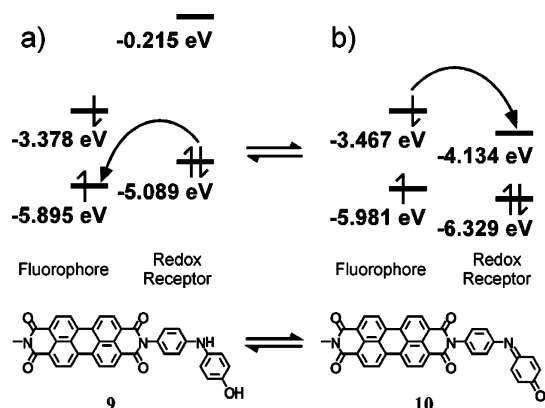


Figure 9. Calculated molecular orbital energies for (a) reduced and (b) oxidized quinonimine-based molecules 9 and 10, showing the quenching mechanism for each.

Experimental Procedures

Material and Methods. NAD⁺, NADH, and yeast alcohol dehydrogenase were purchased from Roche Applied Science. All other chemicals were purchased from Aldrich and used without further purification unless otherwise specified. The acetonitrile used for electrochemical studies was freshly distilled from CaH₂. *N*-(1-Hexylheptyl)perylene-3,4:9,10-tetracarboxyl-3,4-anhydride-9,10-imide (1),^{51,52} 1-(4-aminophenyl)-1,4-dihydronicotinamide (2),^{53–55} 3-(carbamoyl)-1-(2,4-dinitrophenyl)-pyridinium chloride (5),⁵⁶ and 4-hydroxy-4'-nitro-diphenylamine (7)⁵⁷ were synthesized according to the literature methods. Column chromatography was performed on SiliCycle ultrapure silica gel (70–230 mesh). Thin-layer chromatography (TLC) was carried out on Selecto Scientific silica gel 60 F-254 flexible TLC plates. NMR spectra were recorded on a Bruker 300, 400, or 500 MHz instrument as noted, and the chemical shifts were reported relative to TMS at 0 ppm (for ¹H NMR) and CD₃OD at 49.00 ppm (for ¹³C NMR). Atmospheric pressure chemical ionization (APCI) mass spectra were taken on a JEOL JMS-LCmate mass spectrometer (JEOL Ltd., Tokyo, Japan); high-resolution FAB mass spectra were obtained on a JMS HX-110/110A tandem mass spectrometer (JEOL); and matrix assisted laser desorption ionization (MALDI) mass spectra were obtained on a Voyager DE mass spectrometer (AB Biosystems, Framingham, MA). UV/vis absorption spectra were recorded on a Perkin–Elmer Lambda 25 UV/VIS spectrometer and fluorescence emission spectra on a Perkin–Elmer LS 55 fluorometer with excitation at 488 nm. Fluorescence quantum yields were calculated from the integrated emission from 500 to 800 nm over the absorption at 488 nm, relative to *N,N'*-bis(1-hexylhep-

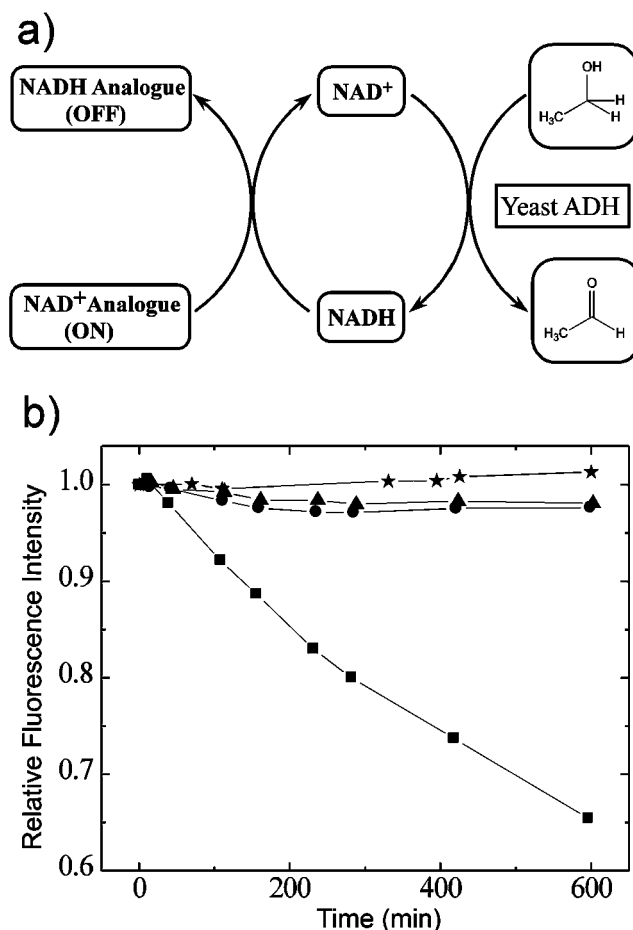


Figure 10. Coupling of the fluorescence switch to the catalytic pathway of alcohol dehydrogenase (ADH): (a) the enzymatic catalytic cycle and (b) experimental realization: the fluorescence is quenched in response to enzymatic reaction (■) while the fluorescence is stable in the absence of either NAD⁺ (●), ADH (▲), or ethanol (★).

tyl)perylene-3,4:9,10-tetracarboxylbisimide in chloroform as a reference ($\Phi_F = 1.0$).⁵⁸

Chemical Redox Switching. Fluorescence was measured in a quartz fluorometer cell with a screw cap (Starna, path length: 10 mm). The fluorescence experiment began with 3 mL of 0.4 μ M NAD⁺ analogue (6) in 2:1 (v/v) CH₂Cl₂/MeOH. For reductions, 4 μ L of 1 mM NaBH₃CN in 2:1 (v/v) CH₂Cl₂/MeOH was added and after 6.5 h at room temperature, and the fluorescence dropped to ~6% of the initial value. For reoxidation, 6 μ L of 4 mM tetrachlorobenzoquinone in 2:1 (v/v) CH₂Cl₂/MeOH was added, and the mixture was exposed to a UV

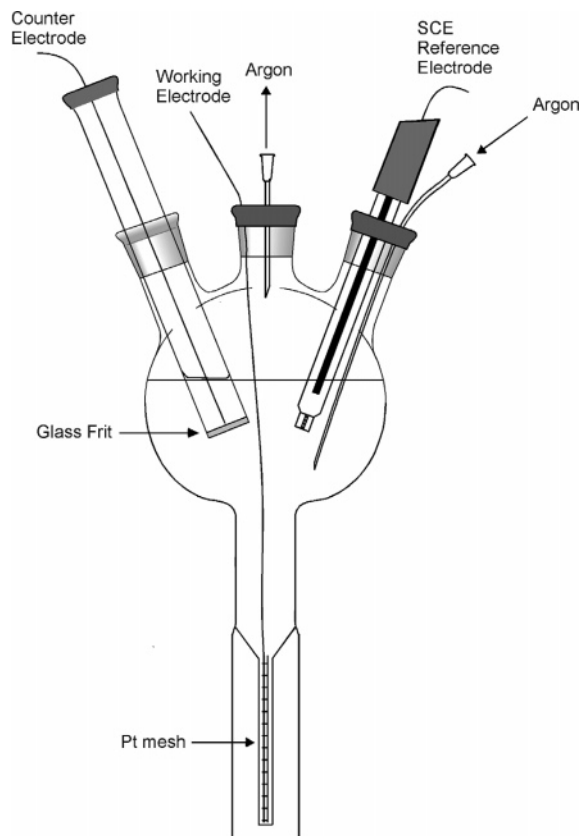


Figure 11. Cell for spectroelectrochemistry.

lamp (UVGL-25, UVP Inc., 366 nm, 18.4 W) for 30 min. For the subsequent switching cycles, the amount of redox reagents used increased gradually: 8 μL of 1 mM NaBH_3CN , 6 μL of 4 mM tetrachlorobenzoquinone, 28 μL of 1 mM NaBH_3CN , and 51 μL of 4 mM tetrachlorobenzoquinone. The ^1H NMR experiment started with 0.55 mL of 1 mM NAD^+ analogue in 1:1 (v/v) $\text{CD}_2\text{Cl}_2/\text{MeOD}$; 10 μL 55 mM NaBH_3CN in 1:1 (v/v) $\text{CD}_2\text{Cl}_2/\text{CD}_3\text{OD}$ was added, and the reaction was complete within 5 min. For reoxidation, 1.5 mg tetrachlorobenzoquinone was added, and the mixture was exposed to UV lamp for 30 min. The tetrachlorobenzoquinone was not completely dissolved but did not affect the spectrum.

Cyclic Voltammetry. Cyclic voltammetry (CV) was carried out using a Model AFRDE5 bi-potentiostat from Pine Instrument Company with data acquisition controlled by in-house written software (Labview, National Instruments). The working compartment contained the analyte in 1:2 $\text{CH}_2\text{Cl}_2/\text{MeCN}$ with 0.1 M NBu_4PF_6 (TBAHFP), a Pt working electrode, and an SCE reference electrode. A silver wire immersed in the same solution was employed as the counter electrode, separated from the working compartment by a glass frit. All potentials were referenced to an internal Fc/Fc^+ couple. The working compartment was purged with argon for 6 min and left under a slight positive pressure of argon during the measurements.

Spectroelectrochemistry. The spectroelectrochemistry was carried out in a 2×10 mm path-length quartz fluorometer cell fused to the bottom of a three-neck flask, with platinum mesh as the pseudo-transparent working electrode (see Figure 11), in a modification of a previously reported setup.⁵⁹ Analyte concentration was 5–10 μM . A thin fluorometer cell (2 mm \times 10 mm) is used so that most of the analyte is confined near the working electrode, and polar solvent (electrolyte in acetonitrile) ensures a fast switching rate. Other conditions were the same

as for the other cyclic voltammetry and fluorescence experiments.

Biochemical Study. The reaction in micellar system was carried out in a Starna cell (4 mm path length) containing 50 mM Tris-HCl buffer (pH = 7.6), 150 mM NaCl, 2.0% *n*-dodecyl- β -D-maltoside (DDM) surfactant, 0.25% cetyltrimethylammonium bromide (CTAB) phase transfer catalyst, 10% (v/v) ethanol, 1.5 mM NAD^+ , and 1.2 μM NAD^+ analogue (**6**). Fifty μL of yeast alcohol dehydrogenase (1 mg/mL) was injected to initiate the reaction, and then the progress was monitored by UV/vis absorption and fluorescence spectra. The reduced product **3** was confirmed by thin-layer chromatography after the solution was evaporated and extracted with CHCl_3 .

Theoretical Methods. Quantum chemical calculations were performed using density functional theory (DFT) in Jaguar 4.1,⁶⁰ at the B3LYP level, with a 6-31G** basis set. Orbitals were visualized in Molden to determine for each orbital whether it was localized primarily on the fluorophore or primarily on the receptor. Solvation was implemented using Jaguar's standard Poisson–Boltzmann dielectric continuum boundary method; settings used were for chloroform (dielectric = 4.806; molecular weight = 119.38; density = 1.4460) for the quinonimine molecules **9** and **10**, and a weighted average of the solvent properties for 2:1 (v/v) $\text{CH}_2\text{Cl}_2/\text{MeOH}$ (dielectric = 25.0; molecular weight = 49.6; density = 0.9822) for the NADH/NAD^+ analogues **3** and **6**. The solution-phase optimized geometries were used for **3** and **6**, as well as for the phenyl-nicotinamide and phenyl-quinonimine model systems, and found to differ only very slightly from the gas-phase optimized geometries, leading to changes of generally <1.5% in the orbital energy levels.

Synthesis of NADH Analogue (3). A total of 6.5 mg (0.03 mmol) of 1-(4-aminophenyl)-1,4-dihydronicotinamide (**2**) and 22.9 mg (0.04 mmol) of *N*-(1-hexylheptyl)perylene-3,4:9,10-tetracarboxyl-3,4-anhydride-9,10-imide (**1**) were mixed in 5 mL of CH_2Cl_2 , and 2 g of imidazole was added. The mixture was heated to 40 $^\circ\text{C}$ under a stream of argon to remove the CH_2Cl_2 , and the solid mixture was heated to 100 $^\circ\text{C}$. The reaction was followed by TLC and was complete \sim 10 min after the imidazole melted. After being cooled, the mixture was dispersed in 5 mL of MeOH, and 90 mL of H_2O was added to precipitate out the product, which was collected by filtration and washed with 30 mL of H_2O . Column chromatography (SiO_2 , 2:98 MeOH/ CH_2Cl_2) gave **3** as a red powder (18 mg, 78%). R_f (silica gel, 5:95 MeOH/ CH_2Cl_2) = 0.25; ^1H NMR (500 MHz, CDCl_3): δ 0.83 (t, 6 H, 2 CH_3), 1.16–1.40 (m, 16 H, 8 CH_2), 1.87 (m, 2 H, α - CH_2), 2.25 (m, 2 H, α - CH_2), 3.26 (br s, 2 H, 4-H nicotinamide), 5.04 (dt, J = 8.1 Hz, 3.3 Hz, 1 H, 5-H nicotinamide), 5.19 (m, 1 H, CH 1-hexylheptyl), 5.24 (s, 2 H, NH_2), 6.45 (d, J = 8.1 Hz, 1 H, 6-H nicotinamide), 7.31 (d, J = 9.2 Hz, 2H, phenylene), 7.34 (d, J = 9.2 Hz, 2 H, phenylene), 7.64 (br s, 1 H, 2-H nicotinamide), 8.65–8.79 (m, 8 H, perylene); MS (MALDI, negative): m/z = 770.96 [M] $^-$ (calc. for $\text{C}_{49}\text{H}_{46}\text{N}_4\text{O}_5$: 770.91).

***N*-(4-Aminophenyl)-*N'*-(1-hexylheptyl)-perylene-3,4:9,10-tetracarboxylbisimide (4).** A total of 100 mg (0.174 mmol) of *N*-(1-hexylheptyl)perylene-3,4:9,10-tetracarboxyl-3,4-anhydride-9,10-imide (**1**), 142 mg of (1.31 mmol) 1,4-phenylenediamine, and 2 g of imidazole was heated at 130 $^\circ\text{C}$ under argon for 5 h. After being cooled, the mixture was dissolved in 100 mL of 1:1 MeOH/ CH_2Cl_2 and then concentrated to about 15 mL to precipitate out the product. The red precipitate was collected by membrane filtration (0.45 μm , Osmonics), washed with 5 mL of MeOH, redissolved in 100 mL of 2:98 $\text{CH}_3\text{COOH}/\text{CH}_2$ -

Cl₂, and stirred at room temperature for 2 h. The solvent was evaporated, and the residue was purified by column chromatography (SiO₂, CHCl₃). Yield 104 mg (90%) *R_f* (silica gel, 5:95 MeOH/CH₂Cl₂) = 0.24; ¹H NMR (500 MHz, CDCl₃): δ 0.83 (t, 6 H, 2 CH₃), 1.16–1.40 (m, 16 H, 8 CH₂), 1.87 (m, 2 H, α-CH₂), 2.25 (m, 2 H, α-CH₂), 3.84 (s, 2 H, NH₂), 5.19 (m, 1 H, 1 CH), 6.84 (d, *J* = 8.4 Hz, 2 H, 2 CH phenylene), 7.11 (d, *J* = 8.4 Hz, 2 H, 2 CH phenylene), 8.63–8.79 (m, 8 H, perylene); HRMS (FAB+): *m/z* = 664.3193 [M+H]⁺ (calc. for C₄₃H₄₂O₄N₃: 664.3175).

NAD⁺ Analogue (6). A solution of 40 mg (0.06 mmol) of the amine **4** in 60 mL of 2:1 CH₂Cl₂/MeOH was added slowly to a solution of 130 mg (0.4 mmol) 3-(carbamoyl)-1-(2,4-dinitrophenyl)-pyridinium chloride (**5**) in 50 mL of dry MeOH in a pressure vessel. After two drops of pyridine (catalyst) was added, the mixture was sealed and stirred at 65 °C for 17 h. After being cooled, the solvent was evaporated, and the residue was purified by column chromatography (SiO₂, 1:10 MeOH/CH₂Cl₂ to elute byproduct and then 2:5 MeOH/CH₂Cl₂ to elute the product). To get rid of small amount of impurity **5**, the solid was dissolved in 40 mL of 1:1 MeOH/CH₂Cl₂, and the solution was concentrated to about 5 mL, at which point the product precipitated out and was collected by membrane filtration (0.45 μm, Osmonics) and washed with 1 mL of MeOH. Yield: 22 mg (41%). *R_f* (silica gel, 1:5 MeOH/CH₂Cl₂) = 0.52; ¹H NMR (500 MHz, 1:1 CD₂Cl₂/CD₃OD): δ 0.85 (t, 6 H, 2 CH₃), 1.19–1.43 (m, 16 H, 8 CH₂), 1.89 (m, 2 H, α-CH₂), 2.28 (m, 2 H, α-CH₂), 5.19 (m, 1 H, 1 CH), 7.85 (d, *J* = 8.4 Hz, 2 H, 2 CH phenylene), 8.07 (d, *J* = 8.4 Hz, 2 H, 2 CH phenylene), 8.45 (t, *J* = 6.8 Hz, 1 H, 5-H nicotinamide), 8.54–8.85 (m, 8 H, perylene), 9.24 (d, *J* = 7.7 Hz, 1 H, nicotinamide), 9.43 (d, *J* = 5.9 Hz, 1 H, nicotinamide), 9.74 (s, 1 H, 2-H nicotinamide); HRMS (FAB+): *m/z* = 769.3439 [M-CI]⁺ (calc. for C₄₉H₄₅O₅N₄: 769.3390).

4-Hydroxy-4'-aminodiphenylamine (8). To a Parr hydrogenator was added 115 mg (0.5 mmol) of 4-hydroxy-4'-nitrodiphenylamine (**7**), 3 mL of methanol, and 10 mg of 10% Pd/C under argon. The system was charged with 40 psi H₂, and the resulting mixture was stirred at room temperature for 18 h. The Pd/C was removed by filtration through Celite, and the solvent was evaporated under reduced pressure. The residue was further purified by column chromatography (SiO₂, 1:9 MeOH/CHCl₃) twice to give a gray powder (76 mg, 76%). *R_f* (silica gel, 1:9 MeOH/CHCl₃) = 0.26; ¹H NMR (500 MHz, CDCl₃): δ 3.47 (s, 2 H, NH₂), 4.33 (s, 1 H, OH), 5.17 (s, 1 H, NH), 6.64 (d, *J* = 8.8 Hz, 2 H), 6.72 (d, *J* = 8.4 Hz, 2 H), 6.83 (d, *J* = 8.4 Hz, 2 H), 6.86 (d, *J* = 8.8 Hz, 2 H). ¹³C NMR (75 MHz, CD₃OD): δ 116.68, 118.16, 120.35, 120.65, 138.97, 139.49, 141.46, 152.10. MS (APCI+): *m/z* = 201 [M+H]⁺.

Hydroquinonimine (9). A total of 40 mg (0.2 mmol) of 4-hydroxy-4'-aminophenylamine (**8**), 57 mg (0.1 mmol) of *N*-(1-hexylheptyl)perylene-3,4:9,10-tetracarboxyl-3,4-anhydride-9,10-imide (**1**), and 2 g of imidazole was stirred at 130 °C under argon for 5 h. After being cooled, the mixture was dispersed in 3 mL of ethanol, acidified to pH = 1 with 2 N HCl, and stirred for 1 h. The red precipitate was collected by vacuum filtration, thoroughly washed with H₂O, redissolved in CH₂Cl₂, and purified by column chromatography (SiO₂, CHCl₃). Yield 28 mg (37%). *R_f* (silica gel, 5:95 MeOH/CH₂Cl₂) = 0.26; ¹H NMR (500 MHz, CDCl₃): δ 0.83 (t, 6 H, 2 CH₃), 1.16–1.40 (m, 16 H, 8 CH₂), 1.87 (m, 2 H, α-CH₂), 2.25 (m, 2 H, α-CH₂), 4.62 (s, 1 H, OH), 5.19 (m, 1 H, 1 CH), 5.66 (s, 1 H, NH), 6.83 (d, *J* = 8.8 Hz, 2 H), 7.02 (d, *J* = 8.4 Hz, 2 H), 7.12 (d, *J* = 8.8 Hz, 2 H), 7.16 (d, *J* = 8.4 Hz, 2H), 8.62–8.79 (m, 8 H,

perylene); MS (MALDI, negative): *m/z* = 755.54 [M]⁻ (calc. for C₄₉H₄₅N₃O₅: 755.34).

Quinonimine (10). To a solution of 15 mg (0.02 mmol) of **9** in 10 mL of CHCl₃, 150 μL of NaClO solution (available Cl₂ 10–13%) was added, and the mixture was stirred at room temperature for 10 min. The solvent was evaporated, and the residue was purified by column chromatography (SiO₂, 0.5:99.5 MeOH/CH₂Cl₂). Yield 5.7 mg (38%). *R_f* (silica gel, 5:95 MeOH/CH₂Cl₂) = 0.51; ¹H NMR (400 MHz, CD₂Cl₂): δ 0.83 (t, 6 H, 2 CH₃), 1.16–1.39 (m, 16 H, 8 CH₂), 1.86 (m, 2 H, α-CH₂), 2.24 (m, 2 H, α-CH₂), 5.17 (m, 1 H, 1 CH), 6.58 (dd, *J* = 10.2 Hz, 2.2 Hz, 1 H, quinonimine), 6.71 (dd, *J* = 10.1 Hz, 2.2 Hz, 1 H, quinonimine), 7.09 (d, *J* = 8.4 Hz, 2 H, phenylene), 7.24 (dd, *J* = 10.2 Hz, 2.7 Hz, 1 H, quinonimine), 7.35 (dd, *J* = 10.1 Hz, 2.7 Hz, 1 H, quinonimine), 7.42 (d, *J* = 8.4 Hz, 2 H, phenylene), 8.59–8.79 (m, 8 H, perylene); MS (MALDI, negative): *m/z* = 753.43 [M]⁻ (calc. for C₄₉H₄₃N₃O₅: 753.32).

Conclusions

We have extended previously developed fluorescent probes based on photoinduced electron transfer¹ to rationally design a new redox switch of fluorescence, featuring a biologically important redox center, by incorporating nicotinamide (the redox center for NAD⁺/NADH) into a fluorophore–spacer–receptor structure. The NAD⁺ analogue was found to be strongly fluorescent ($\Phi_F \approx 1.0$) while the NADH analogue was non-fluorescent ($\Phi_F < 0.001$). Repeated off/on switching of the fluorescence was demonstrated chemically, by reduction with NaBH₃CN and oxidation with tetrachlorobenzoquinone, and electrochemically, over at least 10 cycles with about 13% degradation. Since many proton and metal ion sensors are based on coordination by an amine group, our strategy of replacing a free amine with a nicotinamide group might be a general method to convert other cation sensors to redox switches. We have also shown that ab initio electronic structure calculations of the molecular orbital energy levels accurately predict the observed PET quenching behavior. The potential application of such redox switches as biosensors has also been demonstrated by coupling the switch to the catalytic pathway of yeast alcohol dehydrogenase, a common NADH/NAD⁺-utilizing enzyme.

Acknowledgment. This work was supported primarily by the NSF MRSEC DMR-0213574 and in part by Department of Energy Office of Basic Energy Sciences under the Award Agency Project DE-FG02-02ER15375. D.M.A. thanks Research Corporation for a Cottrell Scholar award RC#CS0937.

Supporting Information Available: ¹H NMR spectra for **3**, **4**, **6**, **8**–**10**. This material is available free of charge via the Internet at <http://pubs.acs.org>.

References and Notes

- Zang, L.; Liu, R.; Holman, M. W.; Nguyen, K. T.; Adams, D. M. *J. Am. Chem. Soc.* **2002**, *124*, 10640.
- Molecular Switches*; Feringa, B. L., Ed.; Wiley-VCH: Weinheim, Germany, 2001.
- Feringa, B. L.; Jager, W. F.; de Lange, B. *Tetrahedron* **1993**, *49*, 8267.
- Irie, M., Ed. Special Issue: Photochromism: Memories and Switches. *Chem. Rev.* **2000**, *100*, 1683–1890.
- Hernandez, R.; Tseng, H.; Wong, J. W.; Stoddart, J. F.; Zink, J. I. *J. Am. Chem. Soc.* **2004**, *126*, 3370.
- de Silva, A. P.; Gunaratne, H. Q.; Gunnlaugsson, T.; Huxley, A. J. M.; McCoy, C. P.; Rademacher, J. T.; Rice, T. E. *Chem. Rev.* **1997**, *97*, 1515.
- Brasselet, S.; Moerner, W. E. *Single Mol.* **2000**, *1*, 17.
- Weiss, S. *Science* **1999**, *283*, 1676.

- (9) Xie, X. S.; Trautman, J. K. *Annu. Rev. Phys. Chem.* **1998**, *49*, 441.
- (10) Bissell, R. A.; de Silva, A. P.; Gunaratne, H. Q. N.; Lynch, P. L. M.; Maguire, G. E. M.; McCoy, C. P.; Sandanayake, K. R. A. S. *Top. Curr. Chem.* **1993**, *168*, 223.
- (11) Aviram, A.; Ratner, M. A. *Chem. Phys. Lett.* **1974**, *29*, 277.
- (12) Carroll, R. L.; Gorman, C. B. *Angew. Chem., Int. Ed.* **2002**, *41*, 4378.
- (13) Adams, D. M.; Brus, L.; Chidsey, C. E. D.; Creager, S.; Creutz, C.; Kagan, C. R.; Kamat, P. V.; Lieberman, M.; Lindsay, S.; Marcus, R. A.; Metzger, R. M.; Michel-Beyerle, M. E.; Miller, J. R.; Newton, M. D.; Rolison, D. R.; Sankey, O.; Schanze, K. S.; Yardley, J.; Zhu, X. *J. Phys. Chem. B* **2003**, *107*, 6668.
- (14) *Fluorescent Chemosensors for Ion and Molecule Recognition*; Czarnik, A. W., Ed.; ACS Symposium Series 538; American Chemical Society: Washington, DC, 1993.
- (15) Probe Design and Chemical Sensing. *Topics in Fluorescence Spectroscopy*; Lakowicz, J. R.; Ed.; Plenum: New York, 1994; Vol. 4.
- (16) de Silva, A. P.; Fox, D. B.; Moody, T. S.; Weir, S. M. *TRENDS Biotechnol.* **2001**, *19*, 29.
- (17) Fabbri, L.; Licchelli, M.; Pallavicini, P. *Acc. Chem. Res.* **1999**, *32*, 846.
- (18) Fabbri, L.; Licchelli, M.; Rabaioli, G.; Taglietti, A. *Coord. Chem. Rev.* **2000**, *205*, 85.
- (19) Tsien, R. Y. *Chem. Eng. News* **1994**, *72*, 34.
- (20) James, T. D.; Sandanayake, K. R. A. S.; Shinkai, S. *Angew. Chem., Int. Ed. Engl.* **1996**, *35*, 1910.
- (21) Tsien, R. Y. *Biochemistry* **1980**, *19*, 2396.
- (22) Burdette, S. C.; Walkup, G. K.; Spingler, B.; Tsien, R. Y.; Lippard, S. J. *J. Am. Chem. Soc.* **2001**, *123*, 7831.
- (23) Walkup, G. K.; Burdette, S. C.; Lippard, S. J.; Tsien, R. Y. *J. Am. Chem. Soc.* **2000**, *122*, 5644.
- (24) Guo, X.; Qian, X.; Jia, L. *J. Am. Chem. Soc.* **2004**, *126*, 2272.
- (25) Nolan, E. M.; Lippard, S. J. *J. Am. Chem. Soc.* **2003**, *125*, 14270.
- (26) Vance, D. H.; Czarnik, A. W. *J. Am. Chem. Soc.* **1994**, *116*, 9397.
- (27) Fabbri, L.; Pallavicini, P.; Parodi, L.; Taglietti, A. *Inorg. Chim. Acta* **1995**, *238*, 5.
- (28) Fabbri, L.; Francese, G.; Licchelli, M.; Perotti, A.; Taglietti, A. *Chem. Commun.* **1997**, 581.
- (29) Nakata, E.; Nagase, T.; Shinkai, S.; Hamachi, I. *J. Am. Chem. Soc.* **2004**, *126*, 490.
- (30) Haugland, R. P. *Handbook of Fluorescent Probes and Research Products*; 9th ed.; Molecular Probes: Eugene, OR, 2002.
- (31) Fabbri, L.; Licchelli, M.; Mascheroni, S.; Poggi, A.; Sacchi, D.; Zema, M. *Inorg. Chem.* **2002**, *41*, 6129.
- (32) Goulle, V.; Harriman, A.; Lehn, J.-M. *J. Chem. Soc., Chem. Commun.* **1993**, 1034.
- (33) Daub, J.; Martin, B.; Knorr, A.; Spreitzer, H. *Pure Appl. Chem.* **1996**, *68*, 1399.
- (34) Li, H.; Jeppesen, J. O.; Levillain, E.; Becher, J. *Chem. Commun.* **2003**, 846.
- (35) Suzuki, T.; Migita, A.; Higuchi, H.; Kawai, H.; Fujiwara, K.; Tsuji, T. *Tetrahedron Lett.* **2003**, *44*, 6837.
- (36) Yee, D. J.; Balsanek, V.; Sames, D. *J. Am. Chem. Soc.* **2004**, *126*, 2282.
- (37) Underwood, A. L.; Burnett, R. W. *Electrochemistry of Biological Compounds*. In *Electroanalytical Chemistry*; Bard, A. J., Ed.; Marcel Dekker: New York, 1973; Vol. 6, p 1.
- (38) Langhals, H. *Heterocycles* **1995**, *40*, 477.
- (39) England, P. A.; Harford-Cross, C. F.; Stevenson, J.-A.; Rouch, D. A.; Wong, L.-L. *FEBS Lett.* **1998**, *424*, 271.
- (40) Imanishi, T.; Hamano, Y.; Yoshikawa, H.; Iwata, C. *J. Chem. Soc., Chem. Commun.* **1988**, 473.
- (41) Rathore, R.; Le Magueres, P.; Lindeman, S. V.; Kochi, J. K. *Angew. Chem., Int. Ed.* **2000**, *39*, 809.
- (42) Gorton, L.; Dominguez, E. *Electrochemistry of NAD(P)+/NAD(P)H*. In *Encyclopedia of Electrochemistry*; Bard, A. J., Stratmann, M., Eds.; Wiley-VCH: New York, 2002; Vol. 9, p 67.
- (43) Elving, P. J. In *Topics in Bioelectrochemistry and Bioenergetics*; Milazzo, G., Ed.; Wiley: New York, 1976; p 179.
- (44) Moracci, F. M.; Liberatore, F.; Carelli, V.; Arnone, A.; Carelli, I.; Cardinali, M. E. *J. Org. Chem.* **1978**, *43*, 3420.
- (45) Anne, A.; Hapiot, P.; Moiroux, J.; Savéant, J.-M. *J. Electroanal. Chem.* **1992**, *331*, 959.
- (46) Salbeck, J.; Kunkely, H.; Langhals, H.; Saalfrank, R. W.; Daub, J. *Chimia* **1989**, *43*, 6.
- (47) Onoda, M.; Uchiyama, S.; Santa, T.; Imai, K. *Anal. Chem.* **2002**, *74*, 4089.
- (48) Miura, T.; Urano, Y.; Tanaka, K.; Nagano, T.; Ohkubo, K.; Fukuzumi, S. *J. Am. Chem. Soc.* **2003**, *125*, 8666.
- (49) Tanaka, K.; Miura, T.; Umezawa, N.; Urano, Y.; Kikuchi, K.; Higuchi, T.; Nagano, T. *J. Am. Chem. Soc.* **2001**, *123*, 2530.
- (50) Langhals, H.; Demmig, S.; Huber, H. *Spectrochim. Acta* **1988**, *44A*, 1189.
- (51) Kaiser, H.; Lindner, J.; Langhals, H. *Chem. Ber.* **1991**, *124*, 529.
- (52) Holman, M. W.; Liu, R.; Adams, D. M. *J. Am. Chem. Soc.* **2003**, *125*, 12649.
- (53) Brewster, M. E.; Kaminski, J. J.; Gabanyi, Z.; Czako, K.; Simay, A.; Bodor, N. *Tetrahedron* **1989**, *45*, 4395.
- (54) Brewster, M. E.; Simay, A.; Czako, K.; Winwood, D.; Farag, H.; Bodor, N. *J. Org. Chem.* **1989**, *54*, 3721.
- (55) Park, K. K.; Han, D.; Shin, D. *Bull. Korean Chem. Soc.* **1986**, *7*, 201.
- (56) Lettre, H.; Haede, W.; Ruhbaum, E. *Liebigs Ann. Chem.* **1953**, 579, 123.
- (57) Halasz, A.; Cohen, D. U.S. Patent 4 021 486 1977.
- (58) Langhals, H.; Karolin, J.; Johansson, L. B.-A. *J. Chem. Soc., Faraday Trans.* **1998**, *94*, 2919.
- (59) Giaimo, J. M.; Gusev, A. V.; Wasielewski, M. R. *J. Am. Chem. Soc.* **2002**, *124*, 8530.
- (60) Jaguar; 4.1, Schrödinger, Inc.: Portland, OR, 2000.